PHYSICAL REVIEW D **85,** 055020 (2012)

Color octet scalars and high p_T four-jet events at the LHC

Jonathan M. Arnold and Bartosz Fornal
California Institute of Technology, Pasadena, California 91125 USA
(Received 15 December 2011; published 23 March 2012)

We study the effect of color octet scalars on the high transverse momenta four-jet cross section at the LHC. We consider both weak singlet and doublet scalars, concentrating on the case of small couplings to quarks. We find that a relatively early discovery at the LHC is possible for a range of scalar masses.

DOI: 10.1103/PhysRevD.85.055020 PACS numbers: 12.60.−i, 14.80.−j

I. INTRODUCTION

If the scalar sector contains colored fields, there are two basic cases—either the scalars can couple to fermions or they cannot. If their gauge quantum numbers forbid couplings to fermions, then in order to enable the new scalars to decay they must be in a real representation of the color gauge group, which allows a cubic coupling in the scalar potential. The lowest dimensional real representation is a color octet. On the other hand, if the new colored scalars can couple to fermions, then one wants to impose minimal flavor violation to forbid tree-level flavor-changing neutral currents. If the new scalars are singlets under the flavor group, then the only representation that can couple to fermions is a color octet. So, there are a number of reasons to focus on the color octet representation.

Color octet scalars appear in many models of new physics currently tested at the LHC. The literature on the subject is vast, covering the case of SU(2) singlets [1–5], as well as doublets [6–11] and triplets [12]. In this paper, we study the effect of color octet scalars on the high transverse momenta four-jet cross section at the LHC. We note that the analysis of multijet events is very promising [1–3,13–17] and may give clues about new physics in the near future.

In the first part of the paper, we concentrate on color octet scalars with no weak quantum numbers. It is a simple extension of the standard model, naturally being anomaly-free and not affected by precision electroweak constraints. The second part concerns weak doublet color octet scalars, namely, the Manohar-Wise model [6]. Our interest in SU(2) doublets is motivated, in part, by the observation that the principal of minimal flavor violation restricts gauge quantum numbers of any scalar sector coupled directly to quarks [6]. The allowed quantum numbers are those of the standard model Higgs doublet, or a color octet scalar with the Higgs weak quantum numbers. In our analysis, we concentrate on cases with small couplings to quarks.

For both weak singlets and doublets, we impose cuts on transverse momenta (p_T) of the jets, which significantly reduces the standard model background. In the singlet case, we implement also restrictions on the invariant mass of jet pairs. We find that, after performing such cuts, the color octet scalar contribution to the four-jet cross section at the LHC is significant in a large region of parameter space. Furthermore, we identify other weak doublet scalar signatures, which may be used to distinguish the doublets from the singlets. However, for those additional processes involving weak doublets, the cross section depends also on other parameters in the scalar potential, which we keep fixed at certain values.

II. WEAK SINGLET SIGNATURE

We begin by investigating the standard model with the addition of SU(2) singlet color octet scalars. Such scalars are coupled to the standard model at tree level only through the $\mathrm{SU(3)_c}$ gauge sector,

$$\mathcal{L}_{\mathrm{kin}} = \mathrm{Tr}[(D_\mu S)^\dagger (D^\mu S)] = \tfrac{1}{2}(\partial_\mu S^a - g_s f^{abc} G^b_\mu S^c)^2. \tag{1}$$

The self-coupling term enabling the scalar decay is

$$\mathcal{L}_{SSS} = -\frac{\mu M_s}{6}\,\mathrm{Tr}(S^3), \tag{2}$$

where M_s is the scalar mass. The complete form of the scalar potential is given in Ref. [1]. Constraints considered there yield $\mu \lesssim 1$.

We are interested in the effects of color octet scalars on the process $pp \to 4\mathrm{jets}$ at the LHC. The cross section for such a process should be modified by the existence of the $pp \to SS \to gggg$ channel. There are four tree-level diagrams contributing to $pp \to SS$ scattering (Fig. 1), while the scalar singlet decay, $S \to gg$, occurs only through loop diagrams (Fig. 2).

The effective scalar-gluon-gluon vertex can be calculated from the diagrams in Fig. 2. The corresponding effective Lagrangian term is

$$\mathcal{L}^{\mathrm{eff}}_{Sgg} = \frac{\mu g_s^2}{128\pi^2 M_s}\left(\frac{\pi^2}{9} - 1\right)\mathrm{Tr}(G_{\mu\nu}G^{\mu\nu}S), \tag{3}$$

where $G_{\mu\nu}$ is the gluon field strength tensor. We note that decays of the weak singlet scalar to quarks (and gluons) can be induced by higher-dimensional operators (for a detailed discussion, see Refs. [2,5]). However, in our analysis we assume that the effect of such operators is negligible.

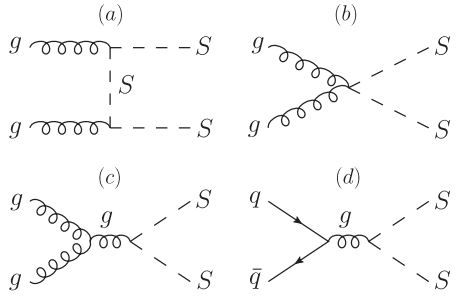

FIG. 1. Feynman diagrams contributing to the $pp \to SS$ scattering.

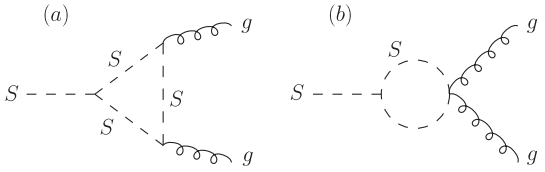

FIG. 2. Diagrams representing color octet scalar decay $S \to gg$.

We expect the impact of SU(2) singlet color octet scalars on the standard model cross section for the process $pp \to 4$jets to be especially pronounced for high p_T four-jet events, where the background is highly suppressed. In addition, appropriate cuts on the invariant mass of jet pairs should further increase the signal-to-background ratio. Our results are summarized in Sec. IV A.

III. WEAK DOUBLET SIGNATURES

The second part of the paper is focused on signatures involving SU(2) doublet color octet scalars. The motivation for such scalars was outlined in the Introduction. A thorough discussion is given in Ref. [6]. Following this reference, we denote the new weak doublet scalar by

$$S^a = \begin{pmatrix} S^{+a} \\ S^{0a} \end{pmatrix}, \tag{4}$$

where $a = 1, \ldots, 8$ is the index of the adjoint color representation. One can split the neutral component of the new doublet into its real and imaginary parts,

$$S^{0a} = \frac{S_R^{0a} + iS_I^{0a}}{\sqrt{2}}. \tag{5}$$

The tree-level masses are [6]

$$\begin{aligned} m_{S^\pm}^2 &= m_S^2 + \lambda_1 \frac{v^2}{4}, \\ m_{S_R^0}^2 &= m_S^2 + (\lambda_1 + \lambda_2 + 2\lambda_3)\frac{v^2}{4}, \\ m_{S_I^0}^2 &= m_S^2 + (\lambda_1 + \lambda_2 - 2\lambda_3)\frac{v^2}{4}, \end{aligned} \tag{6}$$

where m_S is the Lagrangian mass parameter, λ_1, λ_2, λ_3 are dimensionless parameters in the scalar potential, and v is the vacuum expectation value of the standard model Higgs. The full Lagrangian is given in Ref. [6]. Apart from the gauge coupling terms and the scalar potential, one must also consider terms corresponding to the allowed couplings of color octet scalars to quarks. In the quark mass eigenstate basis, the new Yukawa sector becomes

$$\begin{aligned} \mathcal{L} = & -\sqrt{2}\eta_U \bar{u}_R^i \frac{m_U^i}{v} T^a u_L^i S^{0a} \\ & + \sqrt{2}\eta_U \bar{u}_R^i \frac{m_U^i}{v} T^a V_{ij} d_L^j S^{+a} \\ & - \sqrt{2}\eta_D \bar{d}_R^i \frac{m_D^i}{v} T^a d_L^i S^{0\dagger a} \\ & - \sqrt{2}\eta_D \bar{d}_R^i \frac{m_D^i}{v} V_{ij}^\dagger T^a u_L^j S^{-a} + \text{H.c.} \end{aligned} \tag{7}$$

Direct coupling to quarks is an important source of jet production in this model, but it is not the only one. One must also consider decays of S_R^0 to gluon pairs through scalar loops (see Ref. [7]) similar to those in Fig. 2. This time, however, additional decays through quark loops (Fig. 3) are allowed, with the diagram including a top loop contributing the most.

When color octet scalars are coupled to quarks through the Lagrangian terms (7) with large enough η_U, η_D the dominant decay channel (for sufficiently large scalar masses) is to third-generation quarks, giving distinctive $t\bar{t}t\bar{t}$, $t\bar{b}b\bar{t}$, and $b\bar{b}b\bar{b}$ signatures at the LHC (see Ref. [8]). However, when the coupling to quarks is very small, the neutral real component S_R^0 decays predominantly to gluon pairs through scalar loops (the top quark loop contribution becomes negligible in this regime). The effective Lagrangian term describing this decay is

$$\mathcal{L}_{S_R^0 gg}^{\text{eff}} = \frac{3(\lambda_4 + \lambda_5) v g_s^2}{64\pi^2 m_S^2}\left(\frac{\pi^2}{9} - 1\right)\text{Tr}(G_{\mu\nu}G^{\mu\nu}S_R^0), \tag{8}$$

where λ_4, λ_5 are two of the couplings in the scalar potential (see Eq. (6) in Ref. [6]). In addition, the imaginary part of the neutral component S_I^0 and the charged components $S^\pm$ decay through diagrams shown in Fig. 4. We note that the decays $S_I^0 \to Zgg$ and $S^\pm \to W^\pm gg$ can also occur through a scalar loop, but this effect turns out to be negligible.

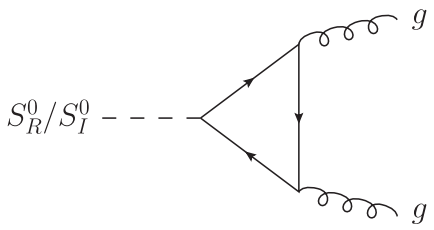

FIG. 3. Diagram for a weak doublet color octet scalar decay to gluons through a quark loop.

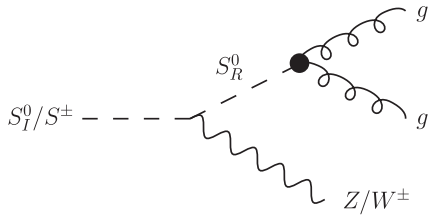

FIG. 4. Tree-level diagram contributing to the weak doublet color octet scalar decays $S_I^0 \to Zgg$ and $S^\pm \to W^\pm gg$.

In the case of small couplings to quarks, the weak doublet color octet scalars are produced similarly as the weak singlets (see Fig. 1), with the scalar pairs being either $S_R^0 S_R^0$, $S_I^0 S_I^0$, $S^+ S^-$, or $S_R^0 S_I^0$. The scalar production in the first three cases has contributions from all diagrams shown in Fig. 1, whereas the last process is described only by the diagram in Fig. 1(b). Each of those cases corresponds to a different LHC signature: 4 jets, $2Z$ + 4jets, W^+W^- + 4jets, and Z + 4jets, respectively. Once again, the signal-to-background ratio can be improved by adopting high p_T cuts.

IV. COLLIDER PHENOMENOLOGY

We used MadGraph/MadEvent [18] (version 1.3.1 of MadGraph 5) to simulate the standard model background and calculate the scalar signal cross section at the LHC running at 7 and 14 TeV center-of-mass energy, for different jet p_T cuts and, in the weak singlet case, cuts on jet pair invariant masses. Apart from this, the default MadGraph run card was used, along with the cteq6L1 parton distribution functions. Jets were ordered by p_T, from highest to lowest. For the simulation of events involving scalars, we used FeynRules [19,20] to generate a model file for MadGraph/MadEvent. Events were run through Pythia and PGS. MadAnalysis was used to plot the results.

We point out that a similar analysis for weak singlet scalars was performed in Ref. [1] using Pythia 5.7. In this paper, however, we improve their analysis by running the events simulated using MadGraph/MadEvent through Pythia 6.420 and PGS4. We also implement a larger set of p_T cuts and impose a slightly different invariant mass cut. In addition, we present plots of the differential cross section as a function of the invariant mass of jet pairs and discuss the current constraints on the color octet scalar masses.

We note that cuts can be tuned based on the scalar mass in order to maximize the effects of the scalars, at the same time leaving a large enough data sample. The restriction on the invariant mass of jet pairs we adopted is

$$\min\left\{\frac{|m_{12} - m_{34}|}{|\max\{m_{12}, m_{34}\}|}, \text{perms.}\right\} < 0.1, \tag{9}$$

where m_{ij} is the invariant mass of the ith and jth jet as ranked by p_T, and "perms." denotes the other two possible pairings of the four jets. This cut simply requires that for at least one of the possible pairings the resulting invariant masses of jet pairs are within 10% of each other. This should significantly suppress the standard model background, whereas the scalar signal is expected to essentially remain unchanged.

It came to our attention, after completing the work on this paper, that the authors of Ref. [21] have also investigated the four-jet signature in search of weak singlet color octet scalars at the LHC. However, apart from using different software in their analysis, they concentrate on a smaller scalar mass range than we do (below 500 GeV) and implement only a single cut on the p_T of the jets for each mass, while we explore a series of such cuts.

A. Weak singlet

Figure 5 shows the four-jet differential cross section as a function of the invariant mass of jets 1 and 4 for various weak singlet color octet scalar masses after adopting the jet invariant mass cut (9) and different p_T cuts. The signal is compared to the standard model background. The cross sections corresponding to several invariant mass windows are given in Table I. In each case, one can calculate the predicted number of events by multiplying the cross section by the integrated luminosity, and estimate the

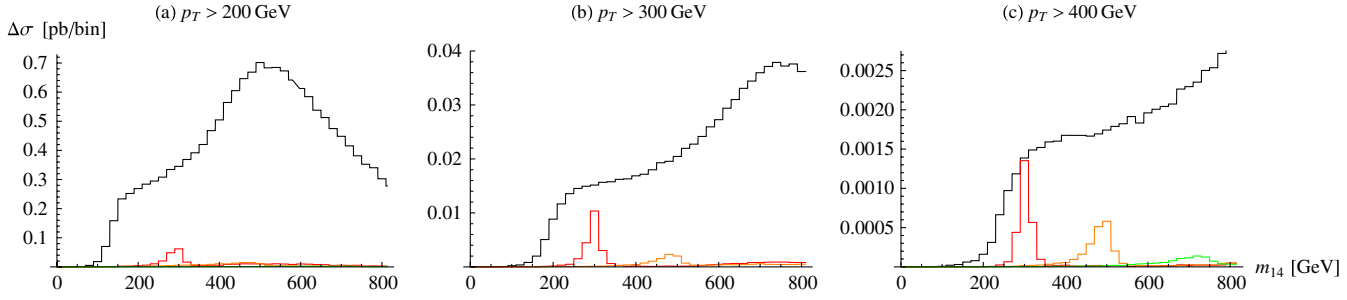

FIG. 5 (color online). The four-jet cross section per bin of the invariant mass of the highest and lowest p_T jets for the invariant mass cut (9) and different p_T cuts: (a) 200 GeV, (b) 300 GeV, and (c) 400 GeV. The black curve is the standard model background. The colored curves: red, orange, and green, correspond to the signal of an SU(2) singlet color octet scalar of mass 300 GeV, 500 GeV, and 750 GeV, respectively. The bin size is 20 GeV.

TABLE I. Cross sections for the weak singlet color octet scalar four-jet signal and the standard model (SM) background in the jet pair invariant mass window $0.9M_s \leq m_{14} \leq 1.1M_s$ for different p_T cuts and scalar masses at $E_{\text{c.m.}} = 14$ TeV.

$p_T^{\min}$[GeV]		M_s 300 GeV	500 GeV	750 GeV	1 TeV
100	σ_S[fb]	1400	160	16	2.4
	σ_{SM}[fb]	1.9×10^5	1.1×10^5	5.3×10^4	3.1×10^4
200	σ_S[fb]	130	47	10	1.8
	σ_{SM}[fb]	1100	3500	3000	1700
300	σ_S[fb]	17	7.0	3.4	1.2
	σ_{SM}[fb]	50	100	290	260
400	σ_S[fb]	2.3	1.6	0.66	0.44
	σ_{SM}[fb]	4.1	8.7	20	42

significance using the standard formula, $S = N_{\text{signal}}/\sqrt{N_{\text{background}}}$.

Figure 6 shows the weak singlet scalar signal significance for different scalar masses and three sample data sizes at 14 TeV LHC center-of-mass energy. We choose $p_T > 200$ GeV since the discovery significance for higher p_T cuts does not improve by much. For scalar masses above 1 TeV, the significance is too small for the signal to be detected with 10 fb^{-1} of data. On the other hand, according to Fig. 6, if there exists a low mass color octet scalar, it should be discovered relatively early at the LHC running at 14 TeV.

We also investigated current LHC constraints on the scalar masses with 1 fb^{-1}, 5 fb^{-1}, and 10 fb^{-1} of data collected at 7 TeV center-of-mass energy. Figure 7 shows the plot of the signal significance in this case as a function of the scalar mass for masses greater than 300 GeV. Those data samples are still too small to extract any constraints on

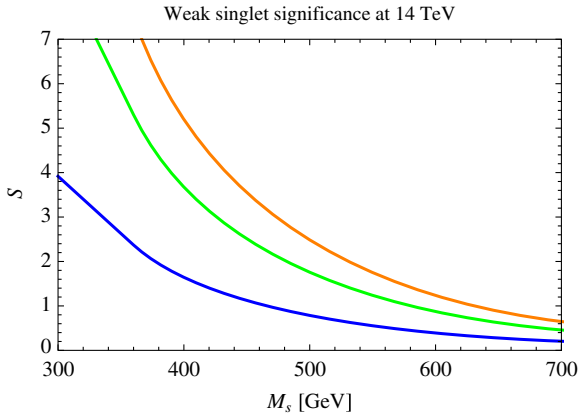

FIG. 6 (color online). The significance of the SU(2) singlet color octet scalar four-jet signal within the invariant mass window $0.9M_s \leq m_{14} \leq 1.1M_s$ as a function of the scalar mass for $E_{\text{c.m.}} = 14$ TeV, $p_T > 200$ GeV, and an integrated luminosity of 1 fb^{-1} (blue), 5 fb^{-1} (green), and 10 fb^{-1} (orange).

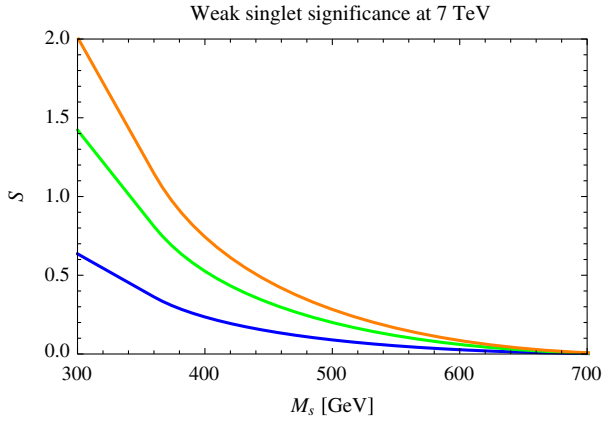

FIG. 7 (color online). Same as Fig. 6, but for $E_{\text{c.m.}} = 7$ TeV.

the color octet scalar masses from the four-jet analysis in this parameter region. However, we note that for lower scalar masses even 1 fb^{-1} of data might be sufficient to set limits on them from the four-jet analysis. In fact, a recent analysis performed using 34 pb^{-1} of data recorded by the ATLAS detector [22] excluded most of the parameter space for weak singlet color octet scalars with masses up to 185 GeV at 95% confidence level.

B. Weak doublet

As was discussed in the previous section, the weak doublet color octet scalar signal depends on the strength of the couplings to quarks. Assuming $\lambda_4 + \lambda_5 \simeq 1$, we find that for η_U, $\eta_D \gtrsim 10^{-6}$ the final states involving heavy quarks overwhelm the $4g$, $2Z + 4g$, $W^+W^- + 4g$, and $Z + 4g$ final states. A detailed analysis of this case can be found in Ref. [8]. On the other hand, when η_U, $\eta_D \lesssim 10^{-8}$, the four final states above become the dominant signatures. In our further analysis, we concentrate on the case of scalars decoupled from quarks, i.e., the limit η_U, $\eta_D \to 0$.

The four-jet signal resulting from the process $pp \to S_R^0 S_R^0 \to gggg$ occurs through the same diagrams as in the weak singlet case (with S_R^0 instead of S). The branching ratio for $S_R^0 \to gg$ is essentially one, therefore, all the results from the weak singlet section, including Figs. 5–7, apply also here. After detecting such a signal, one would need to look for the other three signatures involving weak gauge bosons to distinguish the weak doublet case from the weak singlet color octet scalar signal.

The cross sections for the $2Z + 4$jets, $W^+W^- + 4$jets, and $Z + 4$jets signals depend on the mass parameter m_S, as well as the values of λ_1, λ_2, and λ_3. We emphasis that in our analysis of the SU(2) doublet case we choose particular values of λ_i, i.e., $\lambda_i = 1/2$, for $i = 1, 2, 3$, just to explain how the scalar search method we propose works. There are constraints on λ_i coming from electroweak precision measurements and the requirement that the Higgs quartic

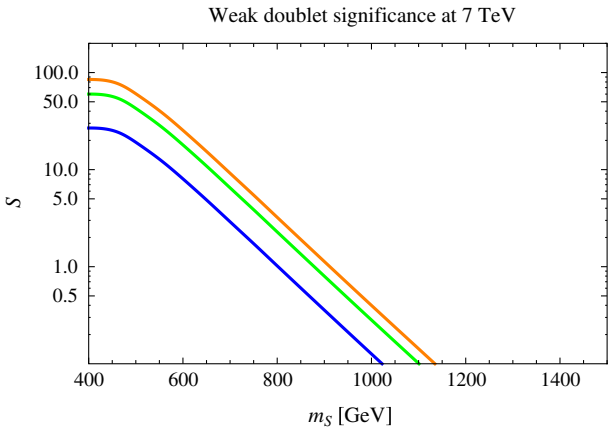

FIG. 8 (color online). The logarithmic plot of the SU(2) doublet color octet scalar $2Z + 4$jets signal significance as a function of the scalar mass parameter m_S for $\lambda_i = 1/2$, $E_{\text{c.m.}} = 7$ TeV, $p_T > 100$ GeV, and an integrated luminosity of 1 fb^{-1} (blue), 5 fb^{-1} (green), and 10 fb^{-1} (orange).

coupling remain perturbative up to some high energy scale (see Ref. [8] for details). The values $\lambda_i = 1/2$ we adopted are consistent with those constraints. The only free parameter remaining is m_S. We note that for our choice of λ_i, the intermediate S_R^0 scalars in the decays $S_I^0 \to ZS_R^0 \to Zgg$ and $S^\pm \to W^\pm S_R^0 \to W^\pm gg$ are off shell.

We find that the cross section for $pp \to S_R^0 S_I^0 \to Z +$ 4jets is negligible compared to the other two processes. Since we choose arbitrary values for λ_i, and because for a given choice of parameters both processes $2Z + 4$jets and $W^+W^- + 4$jets have comparable cross sections, we limit our discussion to the case $pp \to S_I^0 S_I^0 \to 2Z + 4$jets. This channel is very promising since the standard model background is small.

Because of our arbitrary choice of λ_i and the small background, it is natural to expect part of the m_S parameter space to be already excluded by the currently collected data set from the LHC running at $E_{\text{c.m.}} = 7$ TeV. Figure 8 shows the plot of the $2Z + 4$jets signal significance as a function of m_S for the integrated luminosities 1 fb^{-1}, 5 fb^{-1}, and 10 fb^{-1} in this case. Because of the challenge of simulating this standard model background, our analysis was restricted to the parton level, which actually is a good approximation for high jet p_T cuts. A more detailed analysis would have to be done to set firm bounds, however, it is evident that low mass weak doublet color octet scalars are already ruled out (for the particular choice of $\lambda_i = 1/2$) by many sigma. On the other hand, even 10 fb^{-1} of data collected at 7 TeV center-of-mass energy still would not exclude the parameter region $m_S > 900$ GeV.

Table II presents the $2Z + 4$jets scalar signal and the standard model background cross sections for different p_T cuts and a few values of m_S for $E_{\text{c.m.}} = 14$ TeV. Imposing cuts on jet p_T does not improve the discovery significance for $m_S < 800$ GeV, but this parameter region is not interesting since it should already be excluded (for our choice of λ_i). For larger scalar masses, the p_T cuts can increase the significance. For example, in the case of $m_S \simeq 1.5$ TeV the significance increases by a factor of 3 when changing the p_T cut from 100 GeV to 200 GeV, and by a factor of 5 when changing the cut to $p_T > 300$ GeV. Nevertheless, the signal itself drops then below five events for 10 fb^{-1} of data. Figure 9 shows the $2Z + 4$jets signal significance for 14 TeV center-of-mass energy as a function of m_S for a few different integrated luminosities and $p_T > 100$ GeV. According to this plot, if there exists a weak doublet color octet scalar of mass $\sim$1 TeV, it should be discovered relatively early at the LHC running at $E_{\text{c.m.}} = 14$ TeV. With 10 fb^{-1} of data, a discovery of a scalar as heavy as $\sim$1.5 TeV might also be possible. We note that cuts on the invariant mass of jet pairs would increase the significance of the signal, just as in the weak singlet case, but we leave this analysis for a future study.

TABLE II. Cross sections for the weak doublet color octet scalar $2Z + 4$jets signal and the standard model background for different p_T cuts and a few values of m_S at $E_{\text{c.m.}} = 14$ TeV.

$p_T^{\min}$[GeV]	σ_{m_S}[fb]				σ_{SM}[fb]
	500 GeV	750 GeV	1 TeV	1.5 TeV	
100	770	150	24	1.0	7.9
200	18	25	11	0.75	0.48
300	1.5	1.6	2.0	0.43	0.06

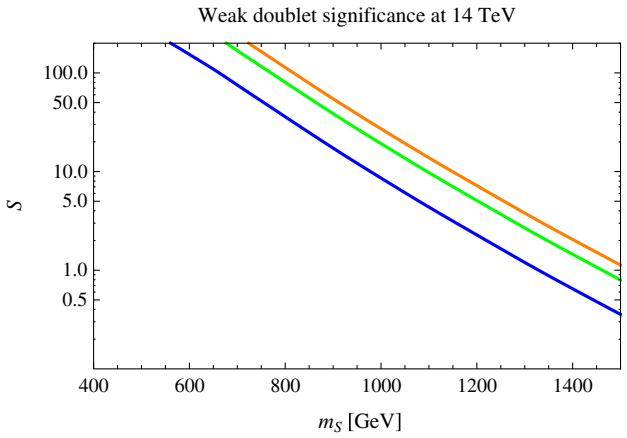

FIG. 9 (color online). Same as Fig. 8, but for $E_{\text{c.m.}} = 14$ TeV.

V. CONCLUSIONS

We have investigated the effect of SU(2) singlet and doublet color octet scalars on high p_T four-jet events at the LHC. We analyzed part of the available parameter space, concentrating on the region least explored so far, i.e., with no couplings or very weak couplings to quarks. We identified the proper signatures in both cases and imposed cuts which improved the signal significance.

In case of weak singlet color octet scalars, one of the best signatures to look for are four-jet events. The standard

model background is significantly suppressed by choosing high transverse momenta jets and cuts on the invariant mass of jet pairs. The signal is then strongly peaked around the invariant jet pair mass equal to the scalar mass. This method can be used to look for low mass scalars already in the first few inverse femtobarns of data from the LHC running at 7 TeV center-of-mass energy.

The same four-jet signature can be used to search for weak doublet color octet scalars with no couplings or very small couplings to quarks. However, in this case there are also other channels involving four jets accompanied by weak vector bosons in the final state. Because the standard model background is extremely small for those additional processes, such channels might be better to look at in search for weak doublet color octet scalars, especially since for massive scalars this signal should be much more significant than the four-jet signal. We performed such an analysis for particular values of the scalar potential parameters. In the case of stronger couplings between the SU(2) doublet scalars and quarks, final states involving bottom and top quarks are more promising channels for discovery.

ACKNOWLEDGMENTS

The authors would like to express their special thanks to Mark Wise for inspirational discussions and many extremely helpful comments at all stages of the work on this paper. We are also very grateful to Johan Alwall for his continuous help, especially concerning the use of the MadGraph 5 software. The work of the authors was supported in part by the U.S. Department of Energy under Contract No. DE-FG02-92ER40701. We further acknowledge the IISN ''MadGraph'' convention 4.4511.10 for access to the UCL cluster. All Feynman diagrams were drawn using JaxoDraw [23].

[1] S. I. Bityukov and N. V. Krasnikov, Mod. Phys. Lett. A **12**, 2011 (1997).
[2] B. A. Dobrescu, K. Kong, and R. Mahbubani, Phys. Lett. B **670**, 119 (2008).
[3] T. Plehn and T. M. P. Tait, J. Phys. G **36**, 075001 (2009).
[4] S. Y. Choi, M. Drees, J. Kalinowski, J. M. Kim, E. Popenda, and P. M. Zerwas, Acta Phys. Pol. B **40**, 1947 (2009).
[5] Y. Bai and B. A. Dobrescu, J. High Energy Phys. 07 (2011) 100.
[6] A. V. Manohar and M. B. Wise, Phys. Rev. D **74**, 035009 (2006).
[7] M. I. Gresham and M. B. Wise, Phys. Rev. D **76**, 075003 (2007).
[8] M. Gerbush, T. J. Khoo, D. J. Phalen, A. Pierce, and D. Tucker-Smith, Phys. Rev. D **77**, 095003 (2008).
[9] C. Kim and T. Mehen, Phys. Rev. D **79**, 035011 (2009).
[10] C. P. Burgess, M. Trott, and S. Zuberi, J. High Energy Phys. 09 (2009) 082.
[11] A. Idilbi, C. Kim, and T. Mehen, Phys. Rev. D **82**, 075017 (2010).
[12] B. A. Dobrescu and G. Z. Krnjaic, arXiv:1104.2893.
[13] R. S. Chivukula, M. Golden, and E. H. Simmons, Phys. Lett. B **257**, 403 (1991).
[14] R. S. Chivukula, M. Golden, and E. H. Simmons, Nucl. Phys. B **363**, 83 (1991).
[15] C. Kilic, T. Okui, and R. Sundrum, J. High Energy Phys. 07 (2008) 038.
[16] C. Kilic, S. Schumann, and M. Son, J. High Energy Phys. 04 (2009) 128.
[17] Y. Bai and J. Shelton, arXiv:1107.3563.
[18] J. Alwall, M. Herquet, F. Maltoni, O. Mattelaer, and T. Stelzer, J. High Energy Phys. 06 (2011) 128.
[19] N. D. Christensen and C. Duhr, Comput. Phys. Commun. **180**, 1614 (2009).
[20] C. Degrande, C. Duhr, B. Fuks, D. Grellscheid, O. Mattelaer, and T. Reiter, arXiv:1108.2040.
[21] S. Schumann, A. Renaud, and D. Zerwas, J. High Energy Phys. 09 (2011) 074.
[22] G. Aad (ATLAS Collaboration), Eur. Phys. J. C **71**, 1828 (2011).
[23] D. Binosi and L. Theussl, Comput. Phys. Commun. **161**, 76 (2004).